
Flexible navigation with neuromodulated cognitive maps

Anonymous Author(s)

Affiliation

Address

email

1

Abstract

2 Animals naturally form personalized cognitive maps to support efficient
3 navigation and goal-directed behavior. In the brain, the CA1 subregion
4 of the hippocampus plays a key role in this process, hosting spatially
5 tuned neurons that adapt based on the behavioral context and internal
6 states. Computational models of this ability include labeled graphs
7 with locally specified spatial information, which avoid global metric
8 structure, and deep neural networks trained on spatial tasks that exhibit
9 emergent spatial tuning. However, these approaches often struggle to
10 model one-shot adaptive mapping and typically rely on plasticity rules
11 that lack biological plausibility.

12 We propose a neural architecture inspired by place-cell dynamics that
13 enables rapid on-the-fly construction of cognitive maps during explo-
14 ration of novel environments. The model relies on velocity inputs and
15 grid cell modules to generate spatial representations and integrates neu-
16 romodulatory signals responsive to boundaries and rewards. Learning
17 combines synaptic plasticity, lateral inhibition, and modulatory gating
18 of place-cell activity. For reward-driven navigation, the agent uses a
19 graph-based algorithm to plan paths on the emergent cognitive map,
20 treating place cells as nodes in a locally structured graph.

21 We tested the model on different environments, achieving high sample
22 efficiency and solving tasks in a single episode, for which usual RL
23 agents require thousands of training steps. This performance advantage
24 arises from biologically inspired inductive biases embedded in the model
25 architecture. In simulation, the agent adapts to dynamic reward locations
26 and changes in the environment layout. Ablation experiments and
27 analysis of neuromodulated place cells reveals task-dependent changes
28 in tuning field size and spatial density, aligning with experimental
29 findings from hippocampal recordings. These results highlight the
30 promise of biologically grounded computation and locally structured
31 graph representations for flexible and data-efficient cognitive mapping.

32

1 Introduction

33 Survival in complex environments requires efficient navigational strategies. From desert ants to
34 humans, successful wayfinding—navigating toward goals that are not directly visible depends on
35 emergent internal spatial representations, known as cognitive maps [1, 2]. Understanding how
36 these maps are constructed from ongoing experiences, and how they can be exploited for flexible
37 goal-directed navigation remains an active area of research in both neuroscience and reinforcement
38 learning (RL).

39 The hippocampus (HP) and entorhinal cortex (EC) serve as the primary neural substrates for spatial
40 representation in the brain. They containing specialized neurons that encode spatial and contextual
41 information—including grid, border, speed, and place cells [3, 4, 5]. Place cells in the CA1 region
42 have attracted particular interest due to their convergence of inputs from periodically tuned grid
43 cells, the CA3 region, and the lateral EC [6, 7, 8, 9]. This strategic integration of diverse spatial and
44 contextual signals suggest CA1 place cells may play a critical role in the formation and maintenance
45 of cognitive maps [10].

46 Another important component are neuromodulators. Their actions include modulation of neuronal
47 dynamics, for instance adjusting the synaptic strength, tuning place fields [11, 12, 13]. Further,
48 neuromodulators such as dopamine transmit reward signals reshaping place cell tuning [14, 15, 16, 17],
49 support novelty detection [12], and encode prediction errors [18, 13], particularly via LEC inputs
50 [19, 20]—mechanisms closely related to reinforcement learning principles.

51 Traditional cognitive map theories propose multiple strategies for spatial navigation based on map-like
52 representations. Route learning encodes paths as sequences of action–position pairs, but it limited
53 in scalability and generalization, especially at route intersections [21, 22, 23]. In contrast, survey
54 maps, which rely on Euclidean geometry, offer greater flexibility [22, 24]; however, their strong
55 geometric assumptions often conflict with neural and behavioral evidence pointing to geometric
56 distortions and topological biases in spatial neural representations [25, 26, 27, 28]. As a middle
57 ground, labeled graphs encode landmarks and transitions within a topological network, enabling
58 vector-like operations, planning, and prediction [29, 30, 31].

59 Computational models have captured some of these aspects individually, showing new ways the
60 brain might use for addressing spatial navigation tasks. Early work proposed that the hippocampus
61 encodes spatial position and direction [32], while topological models based on route learning highlight
62 scalability challenges [23]. More recent approaches draw inspiration from predictive coding and
63 reinforcement learning, including successor representations and the Tolman-Eichenbaum Machine,
64 which generalize across spatial and relational tasks while mimicking biological neural activity patterns
65 [33, 34, 35]. Path integration models trained on velocity inputs give rise to spatial-like receptive fields
66 [36, 37, 38]. Others incorporate reward-driven Hebbian plasticity modulated by neuromodulators
67 [39]. Yet, none of these architectures unify these ingredients into a biologically grounded system that
68 at the same time learns a map of the environment online without relying on an external coordinate
69 system, and flexibility perform goal-directed navigation.

70 In this work, we present a biologically inspired model of cognitive map formation that integrates place
71 cell representations, neuromodulatory signals, and graph-based spatial computations. Our aim is to
72 demonstrate an architecture capable of building a content-rich topological map of the environment on
73 the fly, and leveraging it for efficient, goal-directed navigation—without requiring offline training.

74 Critically, neuromodulators play a central role, as they form analog fields over the map [40], drive
75 local Hebbian plasticity in response to sensory updates [41, 18, 42], and support the formation and
76 adaptation of reward-modulated neural representations used for planning [43, 44, 45, 46, 34]. We
77 show how this system dynamically adapts to environmental changes and how neuromodulation shapes
78 place field allocation and remapping [47, 48], linking cognitive flexibility to underlying physiological
79 mechanisms.

80 The remainder of the paper is organized as follows: Section 2 details the model and experimental
81 setup; Section 3 presents results; Section 4 discusses broader implications and future directions.

82 **2 Methods**

83 We propose a model of cognitive map formation driven by an agent’s experience within a closed
84 environment.

85 The architecture operates with minimal external inputs—limited to binary reward and collision
86 signals—as illustrated in Figure 1a. Instead of relying on exteroceptive cues, spatial representations
87 emerge from idiothetic information, i.e., the agent’s internal perception of self-motion [49], consistent
88 with prior path integration frameworks. Concretely, we use the agent’s ground-truth velocity vector
89 (its actual displacement within the environment) as the primary navigational signal, reflecting the
90 integration of inertial and proprioceptive cues observed in biological systems [50, 51]. Since no
91 visual information is used, the agent is effectively navigating in the dark.

92 **Place Cell Formation** The primary spatial representation is formed by a set of grid cell modules,
 93 each encoding a periodic tiling of 2D space, which directly maps to a toroidal manifold \mathbf{T}^2 (Fig.
 94 1c,d). Departing from traditional grid cell modeling approaches [52, 53], we generate population
 95 activity directly via Gaussian tuning over the torus, continuously updated using the agent’s velocity
 96 vector—an approach validated in prior work [8].

97 The grid cell population vector \mathbf{u}^{GC} is forwarded to a place cell network with initially zeroed synaptic
 98 weights (Fig. 1b). When no place cell is sufficiently active for a given input, a silent unit is randomly
 99 selected and imprinted with the current activity pattern. To enforce representational sparsity and
 100 tuning specificity, lateral inhibition is implemented by comparing the cosine similarity between the
 101 new weight vector and any existing one and a threshold θ_{inh}^{PC} .

102 Each place cell’s activation is computed via a bounded cosine similarity function, determining its
 103 corresponding place field (Fig. 1e). Further implementation details, including lateral inhibition and
 104 recurrent connectivity, are provided in the Appendix.

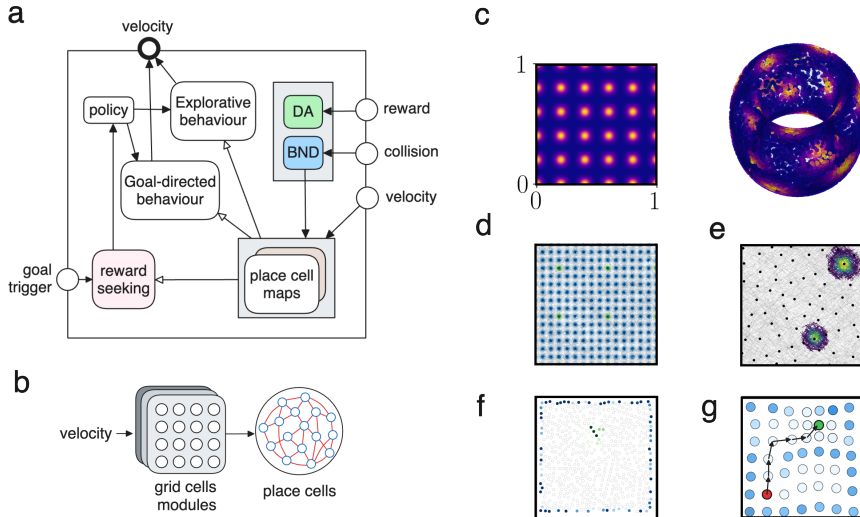


Figure 1: **Model layout and spatial representations** - **a:** the full architecture of the model, consisting of three main sensory input, targeting the two modulators and the cognitive map module, and the executive components, represented by a policy module, two behavioral programs and a reward receiver. **b:** a module of grid cells defined in a bounded square space of length 1, and an activity representation of their receptive field over a torus. **c:** the cognitive map component, organized with a stack of grid cell modules receiving the velocity input and projecting to the layer of place cells. **d:** the neural activity of a grid cell module from a random trajectory; in blue the repeating activity of all cell, while in green the activity of only one, highlighting the periodicity in space. **e:** the distribution in space of the place cells centers, together with the activity of two cells showing the size of their place field. **f:** neuromodulation activity over the place cells map, with in blue the cells tagged by the collision modulation, and in green the ones targeted by reward modulation. **g:** the place cells layer can be regarded as a graph with values assigned to each node according to the modulation strength; a path-finding algorithm can then be used to connect any two nodes taking into account the node values.

105 **Neuromodulation** Neuromodulators deliver event signals: rewards, denoted DA (for dopamine),
 106 and boundary collisions, denoted BND. They are driven by binary inputs and are defined through a
 107 leaky variable with exponential decay.

108 To remain resilient to environmental changes (e.g., moving rewards), the model uses a predictive
 109 mechanism to correct keep internal representations updated. Each modulator k updates synaptic
 110 weights to place cells through Hebbian plasticity:

$$\Delta \mathbf{W}^k = \eta^k \mathbf{u}^{PC} \left(v^k - \mathbf{W}^k \right) \quad (1)$$

111 The term in brackets can be regarded as an error, implementing a simple form of predictive coding
 112 and is inspired by temporal-difference learning [54], aligning with evidence that neuromodulatory
 113 systems signal prediction errors and update beliefs [55, 34, 56].

114 Weight vectors are constrained to remain non-negative. Reward modulation tags cells near rewarded
 115 locations, while boundary modulation builds a representation of environmental edges. These scalar
 116 fields form the core of the cognitive map (Fig. 1f). See Appendix for full learning rules and parameter
 117 settings.

118 **Modulation of Place Fields** We further tested whether neuromodulators could directly alter spatial
 119 tuning. Place fields were dynamically shifted and resized based on recent salience signals.

120 Following a salient event (reward or collision), place field centers were displaced in grid cell space,
 121 with magnitude scaled by the neuromodulator v^k and proximity to the event:

$$\Delta \mathbf{W}_i^{GC,PC} = c^k v^k \varphi_{\sigma^k} (\mathbf{u}^{GC} - \mathbf{W}_i^{GC,PC}) \quad (2)$$

122 Here, φ_σ is a Gaussian function, and c^k a scaling factor. This rule is inspired by BTSP plasticity
 123 [16, 47], which shifts CA1 place fields following salient experiences. Lateral inhibition prevents field
 124 overlap during remapping.

125 In addition to dislocation, field size was modulated by scaling the gain of recently active neurons.
 126 Such mechanism allows neuromodulators to transiently enhance or suppress spatial sensitivity for
 127 specific cells. This modulation rule involves the gain β_i of each cell being adjusted proportionally to
 128 its activity trace m_i , a reference gain constant $\bar{\beta}$, and a modulatory scaling variable:

$$\beta_i = c_a^k m_i \bar{\beta} + (1 - m_i) \bar{\beta} \quad (3)$$

129 where c_a^k is a scaling gain parameter, for which a value of 1. signifies that no modulation takes place.

130 **Policy and Behavior** To evaluate the model’s utility in navigation, we implemented a simple policy
 131 toggling between exploration and goal-seeking behavior, depending on an external goal flag and the
 132 internal map.

133 Exploration consisted of a stochastic walk with persistence, plus periodic plans to visit random known
 134 locations to avoid stagnation. Goal-directed navigation was triggered when a reward representation
 135 was present and executed via shortest-path planning on the place cell graph.

136 The graph was defined by place cells as nodes and synaptic links as edges. The agent selected targets
 137 either randomly or based on cells with high dopaminergic weight, echoing hippocampal replay and
 138 value-based navigation [57, 58, 59]. Planning was achieved via a path-finding algorithm operating
 139 over the graph of place cells. Further, it was introduced also a cost function over the graph nodes
 140 assigning a lower value to boundary cells, with the scope to avoid close proximity to environment
 boundaries, as illustrated in plot 1g.

Table 1: Comparison of neural network models for spatial navigation and representation

Model	Architecture	Training method	Ext. C.
Banino et al. [36]	LSTM + linear layers + CNN	BPTT and deep RL, supervised	Yes
Cueva et al. [38]	RNN + linear layers	Hessian-free algorithm with regularization	Yes
Sorcher et al. [60]	RNN + linear layers	Backpropagation with regularization	Yes
Whittington et al. [35]	Attractor network and deep networks	Backpropagation and Hebbian learning	No
de-Cothi et al. [34]	Successor representation	TD-learning + eligibility traces	Yes
Brozsko et al. [61]	Spike Response Model	Online modulated Hebbian plasticity	Yes
Ours	Rate layers	Online neuromodulated plasticity	No

Model	Task	Input	Output
Banino et al.	Path integration, goal navigation	Velocity, visual input, reward	PC, HDC
Cueva et al.	Path integration	Velocity	Position
Sorcher et al.	Path integration	Velocity	PC
Whittington et al.	Relational graph knowledge	Observation and action	Observation
de-Cothi et al.	Planned navigation	Observation	–
Brozsko et al.	Goal navigation	Position, reward	Action
Ours	Goal navigation	Velocity, reward, collision	Action

Note: PC = Place Cells, HDC = Head Direction Cells, Ext. C. = External Spatial Coordinates

142 **Comparison with previous architectures** Several previous computational models show structural
 143 and conceptual similarities with the present work. A prominent category among them employs deep
 144 neural networks—often with recurrent components—and relies on gradient-based learning strategies
 145 such as backpropagation through time. These models typically require multiple training episodes or
 146 large datasets for convergence. In contrast, our model adopts biologically inspired, synaptically local
 147 plasticity rules, and requires only a single training episode for adaptation.

148 Other models utilize spiking neurons [61] or explicit neural representations [34], and incorporate
 149 online learning rules more closely aligned with ours. These models also focus more directly on
 150 goal-directed navigation, in contrast to purely path integration tasks. However, both of these rely on
 151 external spatial coordinates to represent current position. Our model instead constructs an internal
 152 coordinate system by integrating its own velocity output, enabling endogenous spatial tracking.

153 **Naturalistic task** The model was evaluated on a biologically inspired navigation benchmark
 154 involving exploration and goal-seeking behavior in closed environments. Performance was measured
 155 as the total number of rewards collected over multiple trials.

156 Optimization of the model parameters was carried out using the evolutionary Covariance-Matrix
 157 Adaptation strategy (CMA-ES) [62] with a population of 128 individuals for 100 generations.

158 3 Results

159 **Performance in wayfinding** Our primary aim was to evaluate the formation of the cognitive map
 160 through neuromodulation in terms of the performance of the goal navigation in different environments.

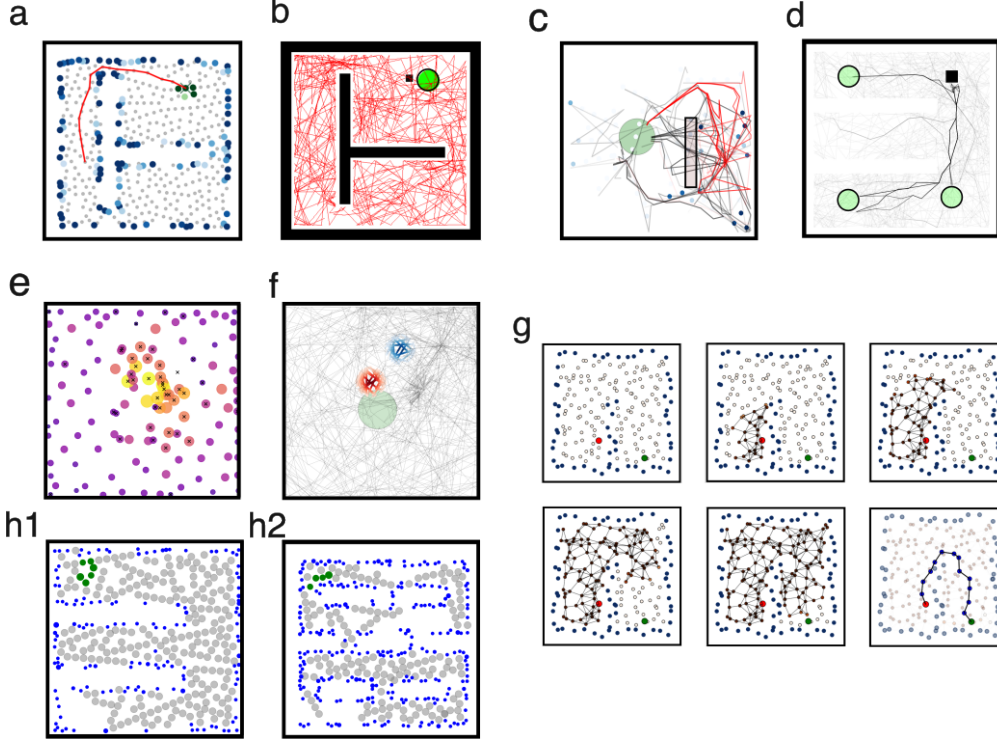


Figure 2: Cognitive maps and performance results - **a:** a cognitive map over a space, together with the plan (red line) to reach a target location from a starting position.. **b:** the same environment but with the reward (green circle), trajectory (red line), agent position (black square). - **c:** plot of trajectories before (black) and after (red) the insertion of a wall (rectangle) between the starting and goal positions, the wall can also be spotted from the boundary cells in blue - **d:** trajectories for multiple trials with the agent starting at the same position (black square) but with the reward location (green circles) periodically moving - **e:** place cells centers with size proportional to their node degree - **f:** place fields of the same cell before and after several relocation of its center following reward events - **g:** visualization of part of the path-finding algorithm, propagation of an activity wave through the place cells network from top-left to bottom-center, and the calculated path visualization in the bottom-right. - **h1-h2:** place cells centers with size inversely proportional to their gain value; in blue boudary cells with the highest average gain, in green reward cells with second smallest gain, the others in grey.

161 The best model resulting from evolution reached solid navigation and adaptation skills. The agent
 162 was able to visit a significant portion of the environment during exploration and use neuromodulation
 163 to produce useful spatial representations.

164 The left panel of plot 2**a-b** displays place cells associated with collisions and reward events, signaling
 165 boundaries (in blue) and reward (in green) locations. The overlap of these two representations and the
 166 non-modulated place cells (in grey) is what we refer to as a cognitive map, since these are the main
 167 sources of spatial and contextual information used during planned navigation, whose path is depicted
 168 as a gray line. The right panel instead portrays the actual environment with walls (black), reward
 169 location (green), and multiple trajectories (red). During exploration, the main areas were visited
 170 until the reward position was located and the goal-directed navigation dominated, as highlighted
 171 by the density of the path lines. Considering the position of the walls and corners, the layout of
 172 this environment does not always make the target locations visible, as it is a non-convex area and
 173 therefore can be classified as wayfinding [63]. The challenge of not being able to use straight lines
 174 is overcome by the graph approach using local data and the consideration of boundary place cells,
 175 allowing the agent to plan accordingly. In addition, considering the Gaussian receptive fields and
 176 the approximately homogenous distribution of place field centers supported by lateral inhibition, the
 177 calculated path accounting for node-length also implicitly minimizes effective path-length, although
 178 not necessarily exactly. Figure 2**g** visualizes part of the path-finding process.

179 In general, this result confirms the ability of the model to focus on navigation and obstacle avoidance.
 180 However, it is worth nothing that not all simulations resulted in a reward being found in the first place,
 181 due to the randomness of the exploratory process; this effect was more pronounced in environment
 182 with more walls and narrow passages.

183 **Detour task** The planning ability and the plastic nature of the cognitive map should provide re-
 184 silience against unexpected changes in the environment layout. In order to verify this we implemented
 185 a detour experiment. Initially, the agent was familiarized with a square environment with the reward
 186 in the middle and starting always from the same position. Then, a wall was placed in between the
 187 starting position and the reward, therefore forcing new trajectory for reaching it. As expected, the
 188 agent was able to form a representation of the new obstacle and calculating new paths around it,
 189 succeeding the task. In plot 2c they are shown the trajectories before and after the wall placement,
 190 and it is manifested the ability of detour in the new layout.

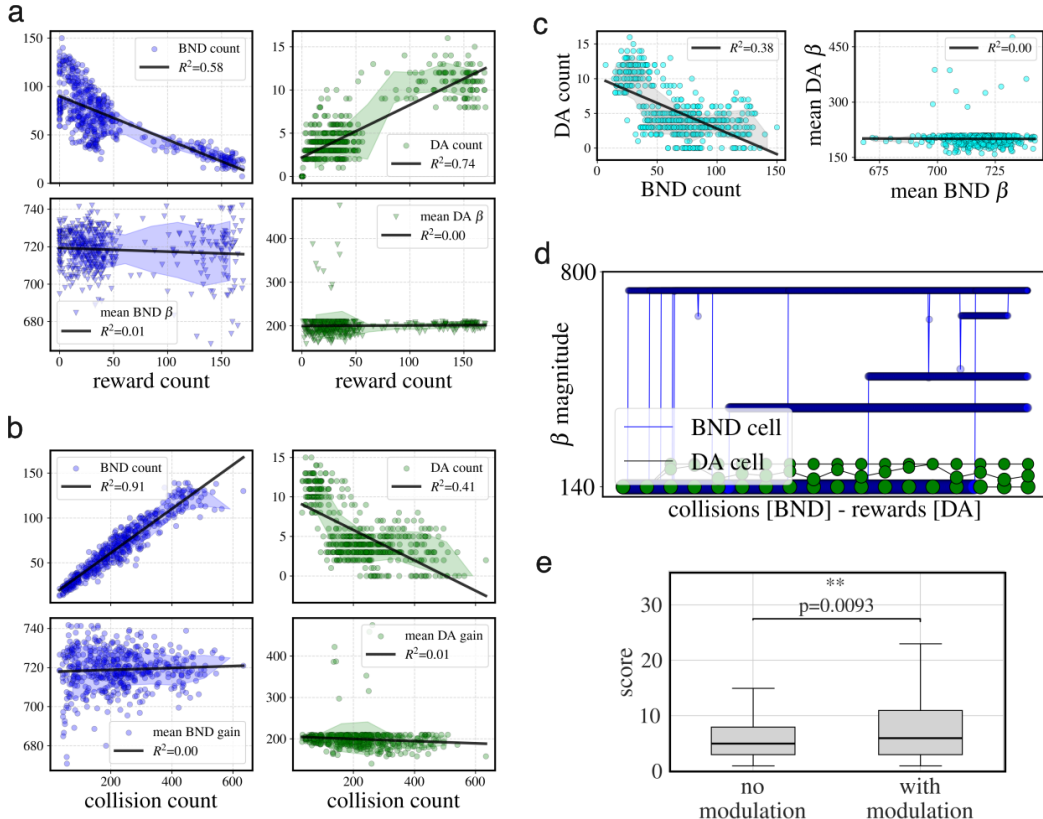


Figure 3: **Cognitive maps and performance results** - **a:** effect of reward count on reward and boundary modulated cells (green and blue respectively), both in total count (top row) and average gain modulation magnitude (bottom row); simulation of 512 independent runs. - **b:** similar plot but with respect to collision count. - **c:** relation between count of reward and boundary modulated cells, and between gain modulation magnitude. - **d:** gain magnitude of boundary and reward cells over sequences of collision and reward events respectively - **e:** performance comparison for the same models on the same environment with and without modulation enabled. Pair-wise t-test over 128 iterations and Bonferroni correction

191 **Adaptive goal representation through sensory error** Then, we tested the adaptability to environ-
 192 mental changes. In this scenario, the reward object was moved after being fetched a fixed number
 193 of times. Here, the difficulty was to unlearning previous locations and discovering new ones, in a
 194 protocol similar to [39]. In plot 2d is reported the set of trajectories over many trials with the reward
 195 displaced in three possible locations. The agent was capable of planning behavior, as earlier, but
 196 also exploring and finding the new rewards, as shown by the density of lines. Whenever a goal path

197 resulted in a failed prediction, the DA-based sensory error weakened the association between the
198 place cells and the reward signal, leading to an extinction of its representation at that location.

199 This result validates the resilience of the model to changing sensory expectations, in this case the
200 reward position.

201 **Modulation of place field size** The construction of model is such that the experience of environmental events can impact the neuronal properties of the generated place cells. In particular, collision and reward events have the effect of affecting the neural activation gain β of BND and DA-modulated cells through an hyperparameter γ . The hyperparameter values c_a^{BND} , c_a^{DA} that yielded the best results were both larger than 1., meaning a shrinking of field size. In plots 2h1-h2 are showed the cognitive maps with relative place field sizes for two environments, showcasing the differences between boundary, reward, and non-modulated cells. in plots 3d is showed the evolution of the gain magnitude for a sample of boundary cells and reward cells over their corresponding modulatory events. Notable is the possible decrease in value, case that occurs when a cell is active but the modulation is absent and the gain thus is pushed down towards the baseline beta. This feature can be considered another adaptation property.

212 **Effect of modulation on performance** Lastly, we investigated the effect of modulating the density
213 of place cells and the size of the field. The goal position was fixed, but the agent was randomly
214 relocated after fetching; performance was defined as the total number of reward counts within a time
215 window.

216 Our working hypothesis is that these experience-driven neuronal changes would improve the quality
217 of the cognitive map and be reflected in navigational abilities. The assessment of this claim was
218 conducted by comparing two variants of the model: with or without the modulation mechanisms,
219 namely the density and gain modulation from reward and collision events.. Both models were ran in
220 the same environment, with numerous wall, for a total of 128 simulations for each case.

221 The statistical results shown in the box plot of Figure 2g demonstrate a significant difference between
222 the two groups, supporting the important of place field modulation.

223 Plot 2e showcases the distribution of place cells with the circle size and color represent the node
224 degree, which aligns discretely with the reward position and the density. Further, in plot 2f the
225 place field of one cell is shown, before and after several reward occurrences and consequent center
226 relocation.

227 Taken together, these findings support the hypothesis of practical utility of direct modulation of
228 place-field structure for active navigation, even in these limited settings.

229 4 Discussion

230 Exploration and planning in the known and past environment are essential behaviors of animals,
231 directly affecting their success in world understanding and goal reaching.

232 An important element behind these abilities is the formation of a map of their surroundings as they
233 make new experiences, known as a cognitive map. Numerous speculations have been made about the
234 shape and neural foundations of such an object, varying in the types of modeling assumptions and
235 experimental support.

236 The contribution of the present work was to propose a rate network model, inspired by the CA1
237 hippocampal region [10]. We used grid cells together with synaptic plasticity as a mechanism to
238 develop information-rich representations based on place cells updated through experience, grouped
239 with common perspectives on cognitive maps [64]. In the spirit of minimizing the geometric
240 assumptions in the neural space, we treated the generated place network as a topological graph, with
241 sensory information added locally through the action of neuromodulators. This idea aligned with the
242 concept of a *labeled graph* [65, 26], however, it is also true that no metric violations were possible in
243 these settings.

244 The tasks we applied the agent to consisted of an exploratory and exploitative phase, in which it was
245 tasked to plan and reach reward positions. For simplicity, the first stage relied on a random walk
246 process, as it was outside the scope of this work. This choice had the side effect that the reward was

247 not always discovered, leading to the formation of incomplete maps, and thus impairing performance.
248 However, this issue was limited in frequency.

249 The simulation results validated the model, showing the expected emergence of cognitive maps and
250 their encoding of information collected during the experience. The online nature of the formation
251 of the locations on the map aligns with the idea of using only idiothetic velocity input, as in path
252 integration [24, 66, 67]. Previous work followed a similar direction using recurrent networks, but
253 required extensive gradient-based training [60, 38, 51]. Another important difference is that our
254 resulting neural network was composed solely of place cells, although neuromodulated, and no other
255 types of neuron were present. This distinction is justified by the partially different task structure, which
256 did not involve supervised learning and did not receive visual information as in [36]. Furthermore,
257 our model relied on predefined grid cells layers, which constituted a strong and sufficient inductive
258 bias, and did not have to be learned from scratch.

259 An additional relevant aspect is also the consideration of the place cell layer as an explicit graph data
260 structure, on which the path-planning and decision-making algorithm was applied. The adoption of
261 this level of description lead to robustness and flexibility, enabling effective navigation in all tested
262 environments, which varying in layout complexity. Nevertheless, this approach did act as another
263 clear inductive bias, which lifted the need to learn an approximation of it through network dynamics
264 and even more differently tuned neurons.

265 Adaptability was tested by occasionally moving the reward position, leading to the generation of
266 an internal prediction error that was used to update its representation on the map. The agent was
267 proved capable of unlearning previous associations, returning to exploration, and memorizing new
268 reward locations. This behavioral protocol is similar to previous work [61], in which dopaminergic
269 and cholinergic activity was utilized within a Hebbian plasticity rule to strengthen or weaken reward-
270 associated spatial representations. However, alternatively to exploiting neuromodulators with opposite
271 valence, we followed a predictive coding framework, a direction linked to hippocampal representations
272 [34, 68] and explored various computational approaches [69, 70, 71]. This choice departed from our
273 focus on using operations on the cognitive map itself by simulating future sensory experiences and
274 learning from feedback. In fact, neuromodulation has been long associated with this functionality
275 [40], especially dopamine [14, 43, 46, 18].

276 Lastly, the hypothesis of the relevance of the active modulation of the neuronal properties of place
277 cells was corroborated by simulating ablation experiments. These tests reported a significant impact
278 of altering the place cells density on the total count of collected rewards. In general, these results are
279 consistent with the experimental observations of alteration of place cells following reward events
280 [16, 72], in particular in terms of increased clustering of cells [73, 74], reminiscent of changes in
281 firing rate after contextual changes [75, 76].

282 Concerning the modulation of place fields, there is significant experimental evidence of their alter-
283 nation during reward events [77, 78, 79], some reporting shrinkage near reward objects [80], and
284 boundaries [81]. The coupling with higher local density could be explained by better optimization of
285 the cell distribution for goal representation and planning [82]. However, in our settings, the fields
286 become enlarged, especially in the direction of the target, although the performance improvements
287 were not tested significantly. A possible explanation can be the simplicity of our reward, which was
288 solely defined as an area of space. The lack of rich non-spatial features thus did not require the place
289 cells to code for smaller spatial variation. Therefore, enlargement might have improved the stability
290 of the representation, marking the nodes associated with rewards more solidly, given the stochas-
291 ticity of its delivery. Further, the graph-path algorithm utilized the strength of the DA-modulated
292 connections for determining the goal representation; stronger fields inherently developed stronger
293 weights, making planning more reliable. Although these findings are limited within the limits of our
294 simulation protocol, there have been experimental observations of elongation of place fields along
295 trajectories over meaningful experiences [83, 84].

296 In conclusion, this work showed a possible architecture for coupling emergent spatial representations
297 with neuromodulated plasticity to achieve an experience-driven cognitive map. The reliance on a few
298 spatial and algorithmic inductive biases, grid cells, and a planning algorithm supports the idea of a
299 label graph for goal navigation. Future work can investigate the application to other spatial domains,
300 such as motor control and three-dimensional navigation. In addition, a richer input feature can be
301 added, such as visual information [85], as well as new neuromodulators that encode different sensory
302 dimensions or internally generated signals.

303

304

305 **Acknowledgements & Statements**

306 The authors declare no competing interests.

307 The code is publicly available and can be found at <https://github.com/iKiru-hub/PCNN>.

308 This research was funded by the European Union's Horizon 2020 research and innovation programme
309 under the Marie Skłodowska-Curie grant agreement № 945371 and the University of Oslo.

310 The research presented in this paper has benefited from the Experimental Infrastructure for Exploration
311 of Exascale Computing (eX3), which is financially supported by the Research Council of Norway
312 under contract 270053.

313 **References**

- 314 [1] Reginald Golledge, Dan Jacobson, Rob Kitchin, and Mark Blades. Cognitive Maps, Spatial
315 Abilities, and Human Wayfinding. *GEOGRAPHICAL REVIEW OF JAPAN SERIES B*, 73:93–
316 104, December 2000.
- 317 [2] Russell A. Epstein and Lindsay K. Vass. Neural systems for landmark-based wayfinding
318 in humans. *Philosophical Transactions of the Royal Society B: Biological Sciences*,
319 369(1635):20120533, February 2014.
- 320 [3] Francesca Sargolini, Marianne Fyhn, Torkel Hafting, Bruce L. McNaughton, Menno P. Witter,
321 May-Britt Moser, and Edvard I. Moser. Conjunctive Representation of Position, Direction, and
322 Velocity in Entorhinal Cortex. *Science*, 312(5774):758–762, May 2006.
- 323 [4] Emilio Kropff, James E. Carmichael, May-Britt Moser, and Edvard I. Moser. Speed cells in the
324 medial entorhinal cortex. *Nature*, 523(7561):419–424, July 2015.
- 325 [5] Trygve Solstad, Edvard I. Moser, and Gaute T. Einevoll. From grid cells to place cells: A
326 mathematical model. *Hippocampus*, 16(12):1026–1031, 2006.
- 327 [6] Daniel Bush, Caswell Barry, and Neil Burgess. What do grid cells contribute to place cell firing?
328 *Trends in Neurosciences*, 37(3):136–145, March 2014.
- 329 [7] Torsten Neher, Amir Hossein Azizi, and Sen Cheng. From grid cells to place cells with realistic
330 field sizes. *PLOS ONE*, 12(7):e0181618, July 2017.
- 331 [8] Tianyi Li, Angelo Arleo, and Denis Sheynikhovich. *Modeling Place Cells and Grid Cells in
332 Multi-Compartment Environments: Hippocampal-Entorhinal Loop as a Multisensory Integra-
333 tion Circuit*. April 2019.
- 334 [9] Olesia M. Bilash, Spyridon Chavlis, Cara D. Johnson, Panayiota Poirazi, and Jayeeta Basu.
335 Lateral entorhinal cortex inputs modulate hippocampal dendritic excitability by recruiting a
336 local disinhibitory microcircuit. *Cell Reports*, 42(1):111962, January 2023.
- 337 [10] Flavio Donato, Anja Xu Schwartzlose, and Renan Augusto Viana Mendes. How Do You Build
338 a Cognitive Map? The Development of Circuits and Computations for the Representation of
339 Space in the Brain. *Annual Review of Neuroscience*, 46(Volume 46, 2023):281–299, July 2023.
- 340 [11] John E. Lisman and Anthony A. Grace. The Hippocampal-VTA Loop: Controlling the Entry of
341 Information into Long-Term Memory. *Neuron*, 46(5):703–713, June 2005.
- 342 [12] Adrian J. Duszkiewicz, Colin G. McNamara, Tomonori Takeuchi, and Lisa Genzel. Novelty
343 and Dopaminergic Modulation of Memory Persistence: A Tale of Two Systems. *Trends in
344 Neurosciences*, 42(2):102–114, February 2019.
- 345 [13] Wolfram Schultz, Peter Dayan, and P. Read Montague. A Neural Substrate of Prediction and
346 Reward. *Science*, 275(5306):1593–1599, March 1997.

- 347 [14] Kimberly A. Kempadoo, Eugene V. Mosharov, Se Joon Choi, David Sulzer, and Eric R.
348 Kandel. Dopamine release from the locus caeruleus to the dorsal hippocampus promotes spatial
349 learning and memory. *Proceedings of the National Academy of Sciences*, 113(51):14835–14840,
350 December 2016.
- 351 [15] Aude Retailleau and Thomas Boraud. The Michelin red guide of the brain: Role of dopamine
352 in goal-oriented navigation. *Frontiers in Systems Neuroscience*, 8, March 2014.
- 353 [16] Katie C. Bittner, Aaron D. Milstein, Christine Grienberger, Sandro Romani, and Jeffrey C.
354 Magee. Behavioral time scale synaptic plasticity underlies CA1 place fields. *Science*,
355 357(6355):1033–1036, September 2017.
- 356 [17] Alexandra Mansell Kaufman, Tristan Geiller, and Attila Losonczy. A Role for the Locus
357 Coeruleus in Hippocampal CA1 Place Cell Reorganization during Spatial Reward Learning.
358 *Neuron*, 105(6):1018–1026.e4, March 2020.
- 359 [18] Denis Sheynikhovich, Satoru Otani, Jing Bai, and Angelo Arleo. Long-term memory, synaptic
360 plasticity and dopamine in rodent medial prefrontal cortex: Role in executive functions. *Frontiers*
361 in *Behavioral Neuroscience*, 16, January 2023.
- 362 [19] Kei M. Igarashi, Hiroshi T. Ito, Edvard I. Moser, and May-Britt Moser. Functional diversity
363 along the transverse axis of hippocampal area CA1. *FEBS Letters*, 588(15):2470–2476, August
364 2014.
- 365 [20] Hiroshi T. Ito and Erin M. Schuman. Functional division of hippocampal area CA1 via
366 modulatory gating of entorhinal cortical inputs. *Hippocampus*, 22(2):372–387, 2012.
- 367 [21] Michael Peer, Iva K. Brunec, Nora S. Newcombe, and Russell A. Epstein. Structuring Knowl-
368 edge with Cognitive Maps and Cognitive Graphs. *Trends in cognitive sciences*, 25(1):37–54,
369 January 2021.
- 370 [22] Elizabeth R. Chrastil and William H. Warren. From Cognitive Maps to Cognitive Graphs. *PLoS
371 ONE*, 9(11):e112544, November 2014.
- 372 [23] Steffen Werner, Bernd Krieg-Brückner, and Theo Herrmann. Modelling Navigational Knowl-
373 edge by Route Graphs. In Christian Freksa, Christopher Habel, Wilfried Brauer, and Karl F.
374 Wender, editors, *Spatial Cognition II: Integrating Abstract Theories, Empirical Studies, Formal
375 Methods, and Practical Applications*, pages 295–316. Springer, Berlin, Heidelberg, 2000.
- 376 [24] C. R. Gallistel and Audrey E. Cramer. Computations on Metric Maps in Mammals: Getting
377 Oriented and Choosing a Multi-Destination Route. *Journal of Experimental Biology*, 199(1):211–
378 217, January 1996.
- 379 [25] Michael Peer, Catherine Nadar, and Russell A. Epstein. The format of the cognitive map
380 depends on the structure of the environment. *Journal of Experimental Psychology: General*,
381 153(1):224–240, January 2024.
- 382 [26] William H. Warren. Non-Euclidean navigation. *Journal of Experimental Biology*,
383 222(Suppl_1):jeb187971, February 2019.
- 384 [27] Mark Wagner. Comparing the psychophysical and geometric characteristics of spatial perception
385 and cognitive maps. *Cognitive Studies: Bulletin of the Japanese Cognitive Science Society*,
386 15(1):6–21, 2008.
- 387 [28] Rainer Rothkegel, Karl F. Wender, and Sabine Schumacher. Judging Spatial Relations from
388 Memory. In Christian Freksa, Christopher Habel, and Karl F. Wender, editors, *Spatial Cognition:
389 An Interdisciplinary Approach to Representing and Processing Spatial Knowledge*, pages 79–
390 105. Springer, Berlin, Heidelberg, 1998.
- 391 [29] Tobias Meilinger. The Network of Reference Frames Theory: A Synthesis of Graphs and
392 Cognitive Maps. In Christian Freksa, Nora S. Newcombe, Peter Gärdenfors, and Stefan Wölfl,
393 editors, *Spatial Cognition VI. Learning, Reasoning, and Talking about Space*, pages 344–360,
394 Berlin, Heidelberg, 2008. Springer.

- 395 [30] Jane X. Wang, Zeb Kurth-Nelson, Dhruva Tirumala, Hubert Soyer, Joel Z. Leibo, Remi Munos,
396 Charles Blundell, Dharshan Kumaran, and Matt Botvinick. Learning to reinforcement learn,
397 January 2017.
- 398 [31] Victor R. Schinazi, Daniele Nardi, Nora S. Newcombe, Thomas F. Shipley, and Russell A.
399 Epstein. Hippocampal size predicts rapid learning of a cognitive map in humans. *Hippocampus*,
400 23(6):515–528, 2013.
- 401 [32] Bruno Poucet. Spatial cognitive maps in animals: New hypotheses on their structure and neural
402 mechanisms. *Psychological Review*, 100(2):163–182, 1993.
- 403 [33] Paul Stoewer, Achim Schilling, Andreas Maier, and Patrick Krauss. Neural network based
404 formation of cognitive maps of semantic spaces and the putative emergence of abstract concepts.
405 *Scientific Reports*, 13(1):3644, March 2023.
- 406 [34] William de Cothi, Nils Nyberg, Eva-Maria Griesbauer, Carole Ghanamé, Fiona Zisch, Julie M.
407 Lefort, Lydia Fletcher, Coco Newton, Sophie Renaudineau, Daniel Bendor, Roddy Grieves,
408 Éléonore Duvelle, Caswell Barry, and Hugo J. Spiers. Predictive maps in rats and humans for
409 spatial navigation. *Current Biology*, 32(17):3676–3689.e5, September 2022.
- 410 [35] James C. R. Whittington, Timothy H. Muller, Shirley Mark, Guifen Chen, Caswell Barry, Neil
411 Burgess, and Timothy E. J. Behrens. The Tolman-Eichenbaum Machine: Unifying Space and
412 Relational Memory through Generalization in the Hippocampal Formation. *Cell*, 183(5):1249–
413 1263.e23, November 2020.
- 414 [36] Andrea Banino, Caswell Barry, Benigno Uria, Charles Blundell, Timothy Lillicrap, Piotr
415 Mirowski, Alexander Pritzel, Martin J. Chadwick, Thomas Degris, Joseph Modayil, Greg
416 Wayne, Hubert Soyer, Fabio Viola, Brian Zhang, Ross Goroshin, Neil Rabinowitz, Razvan
417 Pascanu, Charlie Beattie, Stig Petersen, Amir Sadik, Stephen Gaffney, Helen King, Koray
418 Kavukcuoglu, Demis Hassabis, Raia Hadsell, and Dharshan Kumaran. Vector-based navigation
419 using grid-like representations in artificial agents. *Nature*, 557(7705):429–433, May 2018.
- 420 [37] Ben Sorscher, Gabriel C. Mel, Samuel A. Ocko, Lisa M. Giocomo, and Surya Ganguli. A unified
421 theory for the computational and mechanistic origins of grid cells. *Neuron*, 111(1):121–137.e13,
422 January 2023.
- 423 [38] Christopher J. Cueva and Xue-Xin Wei. Emergence of grid-like representations by training
424 recurrent neural networks to perform spatial localization, March 2018.
- 425 [39] Zuzanna Brzozko, Susanna B. Mierau, and Ole Paulsen. Neuromodulation of Spike-Timing-
426 Dependent Plasticity: Past, Present, and Future. *Neuron*, 103(4):563–581, August 2019.
- 427 [40] Marielena Sosa, Mark H. Plitt, and Lisa M. Giocomo. Hippocampal sequences span experience
428 relative to rewards. *bioRxiv*, page 2023.12.27.573490, February 2024.
- 429 [41] Abdullahi Ali, Nasir Ahmad, Elgar de Groot, Marcel A. J. van Gerven, and Tim C. Kietzmann.
430 Predictive coding is a consequence of energy efficiency in recurrent neural networks, November
431 2021.
- 432 [42] Jacopo Bono, Sara Zannone, Victor Pedrosa, and Claudia Clopath. Learning predictive cognitive
433 maps with spiking neurons during behavior and replays. *eLife*, 12:e80671, March 2023.
- 434 [43] Wolfram Schultz. Dopamine reward prediction error coding. *Dialogues in Clinical Neuroscience*,
435 18(1):23–32, March 2016.
- 436 [44] Jeffrey B. Inglis, Vivian V. Valentin, and F. Gregory Ashby. Modulation of Dopamine for
437 Adaptive Learning: A Neurocomputational Model. *Computational brain & behavior*, 4(1):34–
438 52, March 2021.
- 439 [45] Philippe N. Tobler, Christopher D. Fiorillo, and Wolfram Schultz. Adaptive Coding of Reward
440 Value by Dopamine Neurons. *Science*, 307(5715):1642–1645, March 2005.
- 441 [46] Roshan Cools. Chemistry of the Adaptive Mind: Lessons from Dopamine. *Neuron*, 104(1):113–
442 131, October 2019.

- 443 [47] Aaron D Milstein, Yiding Li, Katie C Bittner, Christine Grienberger, Ivan Soltesz, Jeffrey C
444 Magee, and Sandro Romani. Bidirectional synaptic plasticity rapidly modifies hippocampal
445 representations. *eLife*, 10:e73046, December 2021.
- 446 [48] André A. Fenton. Remapping revisited: How the hippocampus represents different spaces.
447 *Nature Reviews Neuroscience*, 25(6):428–448, June 2024.
- 448 [49] Luxin Zhou and Yong Gu. Cortical Mechanisms of Multisensory Linear Self-motion Perception.
449 *Neuroscience Bulletin*, 39(1):125–137, July 2022.
- 450 [50] Steven J. Jerjian, Devin R. Harsch, and Christopher R. Fetsch. Self-motion perception and
451 sequential decision-making: Where are we heading? *Philosophical Transactions of the Royal
452 Society B: Biological Sciences*, 378(1886):20220333, August 2023.
- 453 [51] Ian Q. Whishaw and Brian L. Brooks. Calibrating space: Exploration is important for allothetic
454 and idiothetic navigation. *Hippocampus*, 9(6):659–667, 1999.
- 455 [52] Yuri Dabaghian. Grid Cells, Border Cells and Discrete Complex Analysis.
- 456 [53] Vemund Sigmundson Schøyen, Kosio Beshkov, Markus Borud Pettersen, Erik Hermansen,
457 Konstantin Holzhausen, Anders Malthe-Sørensen, Marianne Fyhn, and Mikkel Elle Lep-
458 perød. Hexagons all the way down: Grid cells as a conformal isometric map of space. *PLOS
459 Computational Biology*, 21(2):e1012804, February 2025.
- 460 [54] Richard S Sutton and Andrew G Barto. The Reinforcement Learning Problem.
- 461 [55] P. R. Montague, P. Dayan, and T. J. Sejnowski. A framework for mesencephalic dopamine
462 systems based on predictive Hebbian learning. *Journal of Neuroscience*, 16(5):1936–1947,
463 March 1996.
- 464 [56] Seetha Krishnan, Chad Heer, Chery Cherian, and Mark E. J. Sheffield. Reward expectation
465 extinction restructures and degrades CA1 spatial maps through loss of a dopaminergic reward
466 proximity signal. *Nature Communications*, 13(1):6662, November 2022.
- 467 [57] Colin G. McNamara, Álvaro Tejero-Cantero, Stéphanie Trouche, Natalia Campo-Urriza, and
468 David Dupret. Dopaminergic neurons promote hippocampal reactivation and spatial memory
469 persistence. *Nature Neuroscience*, 17(12):1658–1660, December 2014.
- 470 [58] Frédéric Michon, Esther Krul, Jyh-Jang Sun, and Fabian Kloosterman. Single-trial dynamics
471 of hippocampal spatial representations are modulated by reward value. *Current biology: CB*,
472 31(20):4423–4435.e5, October 2021.
- 473 [59] Philip Shamash and Tiago Branco. Mice identify subgoal locations through an action-driven
474 mapping process, December 2021.
- 475 [60] Ben Sorscher, Gabriel Mel, Surya Ganguli, and Samuel Ocko. A unified theory for the origin of
476 grid cells through the lens of pattern formation. In *Advances in Neural Information Processing
477 Systems*, volume 32. Curran Associates, Inc., 2019.
- 478 [61] Zuzanna Brzosko, Sara Zannone, Wolfram Schultz, Claudia Clopath, and Ole Paulsen. Se-
479 quential neuromodulation of Hebbian plasticity offers mechanism for effective reward-based
480 navigation. *eLife*, 6:e27756, 2017.
- 481 [62] Christian Igel, Nikolaus Hansen, and Stefan Roth. Covariance Matrix Adaptation for Multi-
482 objective Optimization. *Evolutionary Computation*, 15(1):1–28, March 2007.
- 483 [63] Tobias Meilinger, Marianne Strickrodt, and Heinrich H. Bühlhoff. Qualitative differences in
484 memory for vista and environmental spaces are caused by opaque borders, not movement or
485 successive presentation. *Cognition*, 155:77–95, October 2016.
- 486 [64] Vincent Hok, Pierre-Pascal Lenck-Santini, Sébastien Roux, Etienne Save, Robert U. Muller,
487 and Bruno Poucet. Goal-Related Activity in Hippocampal Place Cells. *Journal of Neuroscience*,
488 27(3):472–482, January 2007.

- 489 [65] Toru Ishikawa and Daniel R. Montello. Spatial knowledge acquisition from direct experience
490 in the environment: Individual differences in the development of metric knowledge and the
491 integration of separately learned places. *Cognitive Psychology*, 52(2):93–129, March 2006.
- 492 [66] Sabine Gillner and Hanspeter A. Mallot. Navigation and Acquisition of Spatial Knowledge in a
493 Virtual Maze. *Journal of Cognitive Neuroscience*, 10(4):445–463, July 1998.
- 494 [67] Bruce L. McNaughton, Francesco P. Battaglia, Ole Jensen, Edvard I. Moser, and May-Britt
495 Moser. Path integration and the neural basis of the ‘cognitive map’. *Nature Reviews Neuroscience*,
496 7(8):663–678, August 2006.
- 497 [68] Fraser Aitken and Peter Kok. Hippocampal representations switch from errors to predictions
498 during acquisition of predictive associations. *Nature Communications*, 13(1):3294, June 2022.
- 499 [69] Manu Srinath Halvagal and Friedemann Zenke. The combination of Hebbian and predictive
500 plasticity learns invariant object representations in deep sensory networks. *Nature Neuroscience*,
501 pages 1–10, October 2023.
- 502 [70] Alexander Ororbia. Spiking neural predictive coding for continually learning from data streams.
503 *Neurocomputing*, 544:126292, August 2023.
- 504 [71] Kimberly L Stachenfeld, Matthew M Botvinick, and Samuel J Gershman. The hippocampus as
505 a predictive map. *Nature Neuroscience*, 20(11):1643–1653, November 2017.
- 506 [72] Indrajith R. Nair, Guncha Bhasin, and Dipanjan Roy. Hippocampus Maintains a Coherent Map
507 Under Reward Feature–Landmark Cue Conflict. *Frontiers in Neural Circuits*, 16, April 2022.
- 508 [73] Valerie L. Tryon, Marsha R. Penner, Shawn W. Heide, Hunter O. King, Joshua Larkin, and
509 Sheri J. Y. Mizumori. Hippocampal neural activity reflects the economy of choices during
510 goal-directed navigation. *Hippocampus*, 27(7):743–758, July 2017.
- 511 [74] Hannah S Wirtshafter and Matthew A Wilson. Differences in reward biased spatial representa-
512 tions in the lateral septum and hippocampus. *eLife*, 9:e55252, May 2020.
- 513 [75] Michael I. Anderson and Kathryn J. Jeffery. Heterogeneous Modulation of Place Cell Firing by
514 Changes in Context. *Journal of Neuroscience*, 23(26):8827–8835, October 2003.
- 515 [76] Inah Lee, Amy L. Griffin, Eric A. Zilli, Howard Eichenbaum, and Michael E. Hasselmo. Gradual
516 Translocation of Spatial Correlates of Neuronal Firing in the Hippocampus toward Prospective
517 Reward Locations. *Neuron*, 51(5):639–650, September 2006.
- 518 [77] Marianne Fyhn, Sturla Molden, Stig Hollup, May-Britt Moser, and Edvard I. Moser. Hippocam-
519 pal Neurons Responding to First-Time Dislocation of a Target Object. *Neuron*, 35(3):555–566,
520 August 2002.
- 521 [78] P.-P. Lenck-Santini, B. Rivard, R.u. Muller, and B. Poucet. Study of CA1 place cell activity and
522 exploratory behavior following spatial and nonspatial changes in the environment. *Hippocampus*,
523 15(3):356–369, 2005.
- 524 [79] David Dupret, Joseph O’Neill, Barty Pleydell-Bouverie, and Jozsef Csicsvari. The reorgani-
525 zation and reactivation of hippocampal maps predict spatial memory performance. *Nature
526 Neuroscience*, 13(8):995–1002, August 2010.
- 527 [80] S.N. Burke, A.P. Maurer, S. Nematollahi, A.R. Uprety, J.L. Wallace, and C.A. Barnes. The Influ-
528 ence of Objects on Place Field Expression and Size in Distal Hippocampal CA1. *Hippocampus*,
529 21(7):783–801, July 2011.
- 530 [81] Sander Tanni, William De Cothi, and Caswell Barry. State transitions in the statistically stable
531 place cell population correspond to rate of perceptual change. *Current Biology*, 32(16):3505–
532 3514.e7, August 2022.
- 533 [82] Pablo Scleidovich, Jean-Marc Fellous, and Alfredo Weitzenfeld. Adapting hippocampus
534 multi-scale place field distributions in cluttered environments optimizes spatial navigation and
535 learning. *Frontiers in Computational Neuroscience*, 16:1039822, December 2022.

- 536 [83] Mayank R. Mehta, Carol A. Barnes, and Bruce L. McNaughton. Experience-dependent,
 537 asymmetric expansion of hippocampal place fields. *Proceedings of the National Academy of
 538 Sciences*, 94(16):8918–8921, August 1997.
- 539 [84] Jangho Lee, Jeonghee Jo, Byounghwa Lee, Jung-Hoon Lee, and Sungroh Yoon. Brain-inspired
 540 Predictive Coding Improves the Performance of Machine Challenging Tasks. *Frontiers in
 541 Computational Neuroscience*, 16:1062678, 2022.
- 542 [85] John H. Wen, Ben Sorscher, Emily A. Aery Jones, Surya Ganguli, and Lisa M. Giocomo. One-
 543 shot entorhinal maps enable flexible navigation in novel environments. *Nature*, 635(8040):943–
 544 950, November 2024.

545 5 Appendix

546 5.1 Grid cell module

547 It is defined a correspondence between the global environment in which the agent moves, a two-
 548 dimensional Euclidean space \mathbf{R}^2 , and a bounded local space of a grid module, corresponding to a
 549 torus.

550 The global velocity $\mathbf{v} = \{x, y\}$ is then mapped to a local velocity, scaled by a speed scalar s_l^{gc} specific
 551 to the grid cell module l , which determines its periodicity in space.

552 The choice of a toroidal space is motivated by consolidated experimental evidence of the neural space
 553 of grid cells, which are organized in modules of different sizes spanning the animal’s environment.
 554 However, the shape of their firing pattern is known to be hexagonal, which corresponds to the optimal
 555 tiling of a two-dimensional plane, giving rise to a neural space lying on a twisted torus. In this work,
 556 for simplicity, we consider a square tiling and thus a square torus, without much loss of generality
 557 except for the slight increase of grid cells required for a sufficiently cover.

558 A grid cell module l of size N^{gc} is identified by a set of positions defined over a square centered
 559 on the origin and size of 2, such that $\{(x_i, y_i) \mid i \in N^{gc} \wedge x_i, y_i \in (-1, 1)\}$. This local square
 560 space has boundary conditions for each dimension, such that, for instance, when $x_t + s_l^{gc} \cdot v_x > 2$
 561 the position update is taken to the other side $x_{t+1} = x_t + s_l^{gc} \cdot v_x - 2$, where s_l^{gc} is the scale of the
 562 velocity in the local space of the module l with respect to the real global agent velocity $\mathbf{v} = \{v_x, v_y\}$.
 563 When the module is initialized, the starting positions of its cells are uniformly distributed over the
 564 square forming a lattice. When the agent is reset in a new position at the beginning of new trial, a
 565 displacement vector is applied to the last cells positions such that the mapping between the module
 566 local space and the global environment is preserved.

567 The firing rate vector of each cell is determined with respect to a 2D Gaussian tuning curve centered
 568 at the origin at $(0, 0)$, and it is calculated as

$$569 r_i = \exp\left(-\frac{x_i^2+y_i^2}{\sigma_l^{gc}}\right), \text{ where } \sigma_l^{gc} \text{ is the width of the tuning curve for module } l. \text{ An illustration of the}\\
 570 \text{receptive field over a 2D environment and a toroidal space is reported in Figure 4a-b.}$$

571 The final population vector of the grid cell network GC is the concatenated and flattened firing rate
 572 vector of all modules \mathbf{u}_l^{GC} .

573

574 In our model, each grid cell had a tuning width of 0.04. They were defined as 8 modules of size 36,
 575 and the relative speed scales were $\{1., 0.8, 0.7, 0.5, 0.4, 0.3, 0.2, 0.1, 0.07\}$.

576 5.2 Place cells

577 **Tuning formation** The tuning of a new place cell is simply defined as the current GC population
 578 vector \mathbf{u}_l^{GC} , and its index is that of the first silent cell, which is added to the forward weight matrix
 579 $\mathbf{W}_i^{GCToPC} \leftarrow \mathbf{u}_l^{GC}$.

580 In order to avoid overlapping of place fields, lateral inhibition is implemented. More specifically, the
 581 tuning process is aborted in case the cosine similarity of the new pattern and the old ones is greater
 582 than a threshold θ_{inh}^{PC} .

583 Each cell represents a position in the GC activity space, which can be considered a node within a
 584 graph of place cells (PC). Although it is totally possible to only use the N^{GC} -dimensional tuning
 585 patterns and be agnostic about the dimensionality of the space in which the agent lives, to simplify
 586 the calculations, we mapped each pattern to 2D positions in a vector space. Then, the PC recurrent
 587 connectivity matrix is calculated with a nearest neighbors algorithm, which instead of a fixed number
 588 K of neighbors uses a lateral distance threshold θ_{rec}^{PC} .

589 **Activity** The current firing rate of the PC population is determined by the cosine similarity between
 590 the GC input and the forward weight matrix, then passed through a generalized sigmoid $\phi(z) =$
 591 $[1 + \exp(-\beta(z - \alpha))]^{-1}$. The parameter α represents the activation threshold, or horizontal offset,
 592 while β the gain, or steepness.

$$u_i^{PC} = \phi \left(\cos \left(u^{GC}, W_i^{GC,PC} \right) \right) \quad (4)$$

593 It is also defined as an activity trace, which has an upper value of 1 and decays exponentially:

$$m_i = -m_i/\tau^{PC} + u_i \quad (5)$$

594 It is used as a proxy for a memory trace.

595
 596 In the model, a PC population is defined by its average place field size, determining the granularity
 597 of the representation of the place. In plot 4b it is illustrated an example of place cells layer tuning
 598 obtained from a continuous trajectory over a square environment.

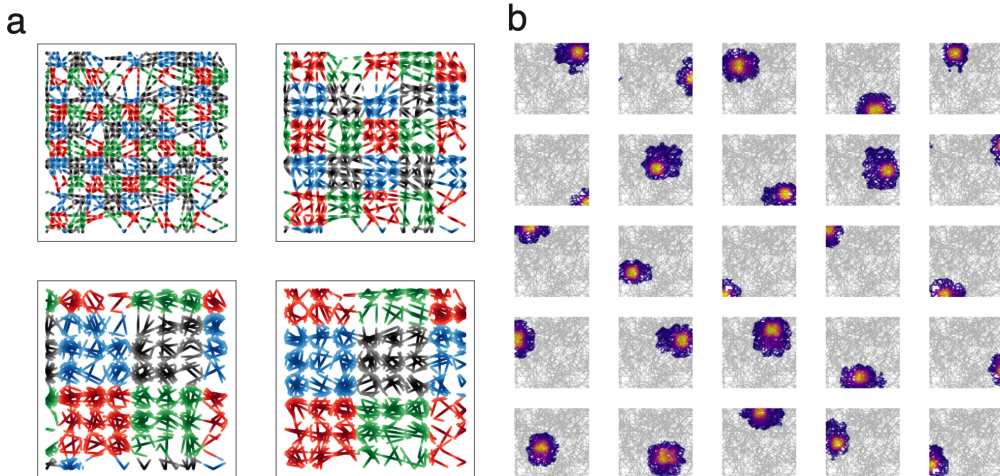


Figure 4: **Place fields obtained from grid cells activity** - **a:** grid cell modules with different granularity represented over a continuous trajectory in an open space. For visualization purposes, each module is represented as composed of four sub-modules of 9 grid cells each, whose periodic tuning generates activity that repeats in space. **b:** place cells whose spatial tuning has been obtained from the concatenation of the grid cells population vector.

599 5.3 Modulation

600 Neuromodulation is implemented as a reward-sensitive signal, represented as DA (mimicking the
 601 function of dopamine), and a collision-sensitive signal, represented as BND (for boundary). Its
 602 dynamics are defined in terms of a leaky variable v whose state is perturbed by an external input x ,
 603 whose qualitative meaning differs for each neuromodulator k .

$$\begin{aligned} v^k &= -v^k/\tau^k + x^k \\ v^k &= \max(v^k, 0) \end{aligned} \quad (6)$$

604 $\tau_{DA} = 2, \tau^{BND} = 1$

605 **Learning rule** The connection weights \mathbf{W}^k are updated according to a plasticity rule composed of
 606 an Hebbian term, involving the leaky variable, the place cells that are above a certain threshold θ^k ,
 607 and the current connection weights value:

$$\Delta \mathbf{W}^k = \eta^k \mathbf{u}^{PC} (v^k - \mathbf{W}^k) \quad (7)$$

608 where the weight contribution of the Hebbian update, and η^k is the learning rate: $\eta^{DA} = 0.9, \eta^{BND} =$
 609 0.9. Additionally, connections values are kept non-negative.

610 **Active neuronal modulation** Neuromodulation acts on the neuronal profile of the place cells by
 611 affecting the value of the activation gain and relocate the center of their tuning.

612 Gain modulation is implemented using the activity traces and a constant reference gain value $\bar{\beta}$:

$$\beta_i = c_a^k m_i \bar{\beta} + (1 - m_i) \bar{\beta} \quad (8)$$

613 where c_a^k is a scaling gain parameter, and if it is 1 then no modulation takes place.

614 Concerning center relocation, it is applied to recently active neurons with non-zero trace m_i . For a
 615 place cell i with position \mathbf{x}_i (in the vector space), it is calculated a displacement vector \mathbf{q}_i with respect
 616 to the current position \mathbf{x}_j , identified as the most active place cell j .

$$q_i = c_b^k v^k \exp\left(-\frac{\|\mathbf{x}_i - \mathbf{x}_j\|}{\sigma^k}\right) \quad (9)$$

617 where c_b^k is a scaling relocation parameter, while σ^k the width of the Gaussian distance. This
 618 displacement is used to move in GC activity space and get the new GC population vector to use as
 619 tuning pattern.

620 Also in this case, it is ensured that the new place field center is at a minimum distance θ_{min}^{PC} from the
 621 others; here Euclidean distance is used.

622 5.4 Decision making

623 Behaviour selection logic

624 The possible behaviours are *exploration* and *exploitation*, and an action is defined as a 2D velocity
 625 vector. For exploration, an action can be generated either as random navigation, using a polar vector
 626 of fixed magnitude (the speed) and angle sampled from a uniform distribution, or as a step within
 627 a goal-directed navigation plan to reach a random destination, which corresponds to a randomly
 628 sampled existing place cells. In the goal-directed navigation the magnitude of the velocity vector
 629 is less or equal than a fixed speed value, depending on the distance from the next target position in
 630 the plan. Instead, for the exploitation behaviour, the action is a step within a goal-directed navigation
 631 towards the reward location. The behaviour selection process depends on the experience of collision,
 632 the presence of a plan, and the success in the navigation planning. A diagram of this logic is reported
 633 in Figure 5.

634 The positions of the agent and of the target location for planning are identified by the place cells
 635 population vector. In particular, the reward position (x_r, y_r) is determined by the weighted average of
 636 the centers x_i, y_i of the place cells with respect to their DA-modulated connections weights. Further,
 637 only the top 5 place cells are considered.

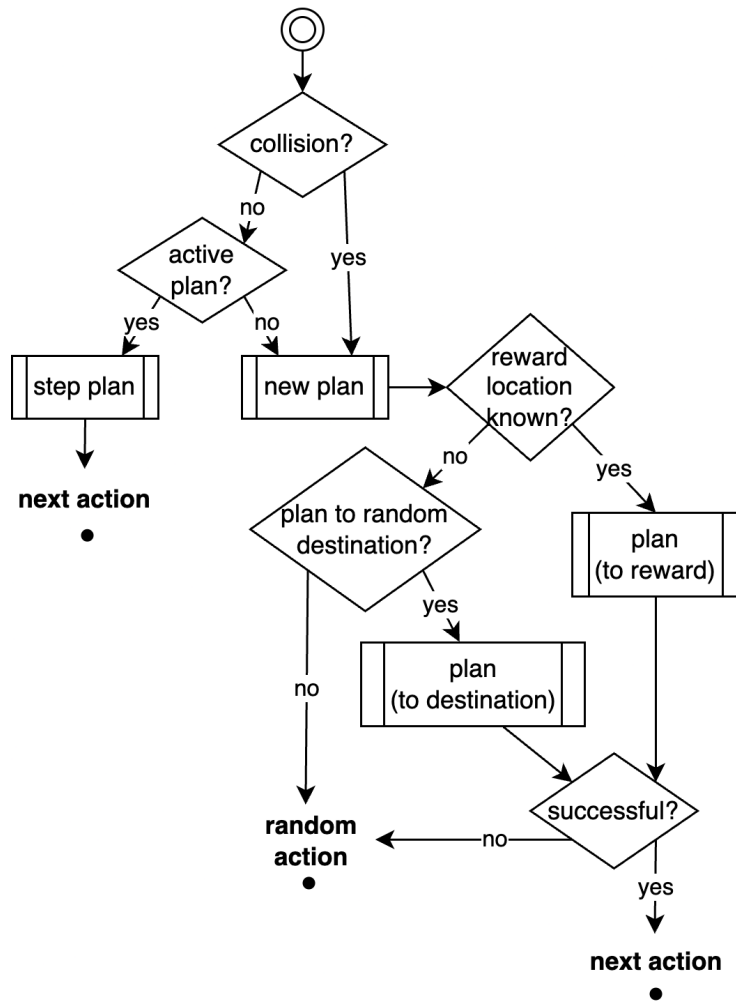


Figure 5: Diagram of the behaviour selection process

$$x_r = \sum_i^5 W_i^{DA} x_i$$

$$y_r = \sum_i^5 W_i^{DA} y_i$$
(10)

Algorithm 1 ACTIVITY-BASED PATHFINDING

Require: Connectivity matrix $C \in \mathbb{R}^{n \times n}$, node weights $w \in \mathbb{R}^n$, start node s , end node e

Ensure: A list of nodes forming a (short) path from s to e , or empty if none found

```

1: Initialize activity vector  $a \leftarrow \mathbf{0} \in \mathbb{R}^n$ ; set  $a_s \leftarrow 1$ 
2: Initialize history list  $H \leftarrow []$                                  $\triangleright — Forward propagation phase —$ 
3: for  $t = 1$  to  $\text{MAX\_PATH\_DEPTH}$  do
4:    $a \leftarrow C \cdot a$ 
5:    $a \leftarrow a \circ w$                                                $\triangleright \text{Element-wise multiplication with node weights}$ 
6:    $a \leftarrow \sigma(4(a - 0.6))$                                       $\triangleright \text{Apply sigmoidal activation: } \sigma(x) = \frac{1}{1+e^{-x}}$ 
7:    $a_i \leftarrow 0$  if  $a_i < 0.1$  (thresholding)
8:   Append  $a$  to  $H$ 
9:   if  $a_e > 0$  then
10:    break
11:   end if
12: end for
13: if maximum depth reached then
14:   return []                                                        $\triangleright \text{No path found}$ 
15: end if
16: if  $|H| < 3$  then
17:   return  $[s, e]$                                                $\triangleright \text{Path is trivially short}$ 
18: end if
19: Initialize path index stack  $G \leftarrow [[e]]$ 
20: for  $t = 1$  to  $\text{MAX\_PATH\_DEPTH}$  do
21:   Let  $m \leftarrow C_G[t-1]$                                           $\triangleright \text{Get neighbors of current group}$ 
22:   if  $m_s > 0$  then
23:     break
24:   end if
25:    $a \leftarrow H[-(t+1)] \circ m$ 
26:   Append  $\{i : a_i > 0\}$  to  $G$ 
27: end for                                                  $\triangleright — Path reconstruction —$ 
28:  $P \leftarrow [e]$ 
29: for  $t = 1$  to  $|G| - 1$  do
30:   Initialize  $a \leftarrow \mathbf{0} \in \mathbb{R}^n$ 
31:   Set  $a_i \leftarrow 1$  for all  $i \in G[t]$ 
32:    $a \leftarrow a \circ C_P[-1]$ 
33:   if  $\sum a = 0$  then
34:     return []                                                        $\triangleright \text{No valid neighbor}$ 
35:   else
36:     Choose  $j \in \{i : a_i > 0\}$  uniformly at random
37:     Append  $j$  to  $P$ 
38:   end if
39: end for
40: Append  $s$  to  $P$ 
41: return  $\text{reverse}(P)$ 

```

640 The planning of a new route is implemented as a path-finding algorithm based on the place cell graph,
641 provided as connectivity matrix C . Its particularity is the use of a weighting \tilde{W} of the nodes according
642 to the neuromodulation map. A description is reported in algorithm 5.4.

643 **5.5 Environments**

644 The game in which test the model has been developed with the python library Pygame, used under
645 license GNU LGPL version 2.1 and available at <https://github.com/pygame/pygame>. The
646 environment layout consisting in a customizable arrangement of vertical and horizontal hard walls
647 with variable length and fixed width. Below in Figure 6 some samples are shown.

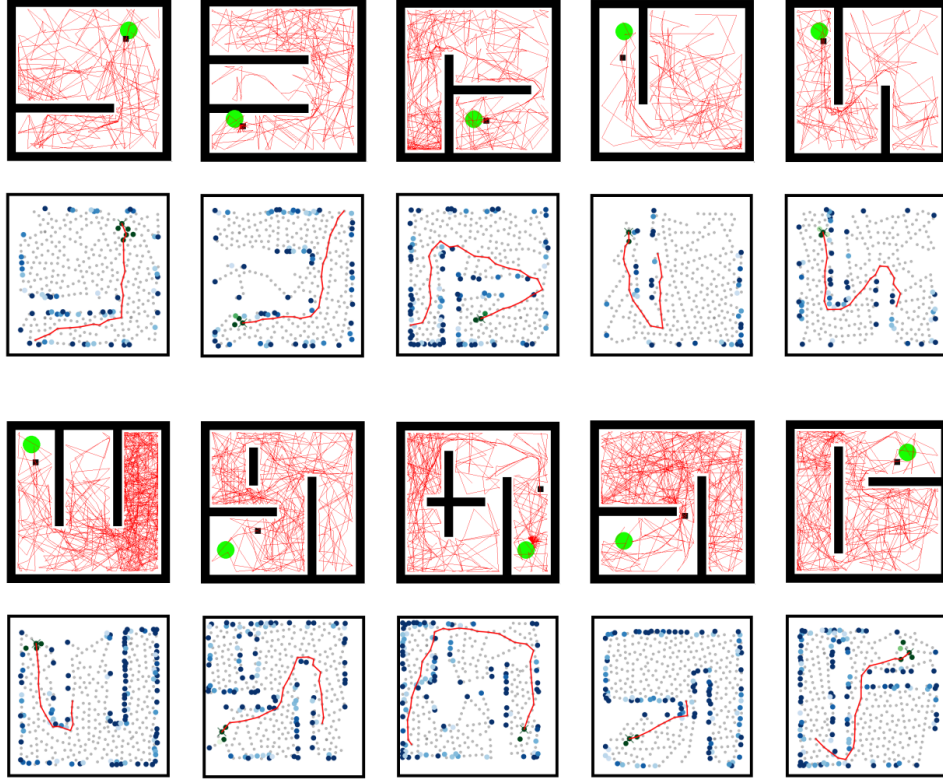


Figure 6: Sample of generated environments

648 The reward object is defined as a circle with size the 5% of the total environment area. When the
 649 agent position is within its boundary, it is provided a binary signal $R \sim \mathcal{B}(p_r)$ drawn from a Bernoulli
 650 with probability $p_r = 0.6$. The duration of the reward fetching is set to 2 time steps.

651 The agent object is defined as a square with size the 3.3% of the total environment area.

652 The testing protocol was inspired by the behavior of animals that venture into new territories in search
 653 of food. It was divided into two parts:

- 654 • **exploration phase:** the agent was placed in a random location within the environment for
 655 10'000 time steps. In this phase the reward is not present. Further, in order to force greater
 656 exploration of the environment, every 3'000 steps it was teleported to another random
 657 location. This external intervention was meant to mitigate the randomness in the exploratory
 658 behavioural strategy of the agent.
- 659 • **reward phase:** a reward is insert in a random location, and it is available to be discovered.
 660 When it is encountered, the agent is teleported to a random location within the environement,
 661 and after a fixed about 100 time step it is enabled its reward-seeking behaviour, in the form
 662 of goal-directed navigation. The total duration of this phase is set to 20'000 time steps.

663 An episode is defined as a continuous trajectory during the reward phase, namely a set of time steps
 664 starting from when the agent is place in a position until either it finds the reward or the simulation
 665 ends.

666 **Detour experiment** The protocol is modified such that after a fixed number of episodes the layout
 667 of the environment is changed, e.g. a wall is inserted. This experiment is meant to test the ability
 668 to reach the reward location by using the same cognitive map, and possibly update it with the new
 669 sensory information, such as the detection of the new boundaries.

670 **Changing reward experiment** During the reward phase, the reward location is changed after a
 671 fixed number of fetches.

672 **Optimization** The model hyper-parameters such as the constants for the neural dynamics and
 673 the behaviour selection have been optimized through a evolutionary algorithm. Initially, an initial
 674 population of individuals with different random genomes (string of hyper-parameters values) is
 675 evaluated according to a fitness function, in this case a set of different environments.

676 Next, the population of a new generation is constructed from the first by combining and mutating the
 677 genomes of the top ranked individuals from the previous generation.

678 In particular, we used the Covariance Matrix Adaptation algorithm, in which the shape of distribution
 679 of genome values is iteratively adapted according to the recent performances.

680 The evolved hyper-parameters are: neural gain β , lateral inhibition threshold θ_{inh}^{PC} , lateral distance
 681 threshold θ_{rec}^{PC} , activity trace time constant τ^{PC} , reward modulation scale c_b^{DA} , reward modulation
 682 spread x_b^{DA} , boundary modulation scale c_b^{BND} , boundary modulation spread c_b^{BND} , reward gain
 683 modulation c_a^{DA} , and boundary gain modulation c_a^{BND} . The distribution of the genome values is
 684 reported in Figure 7.

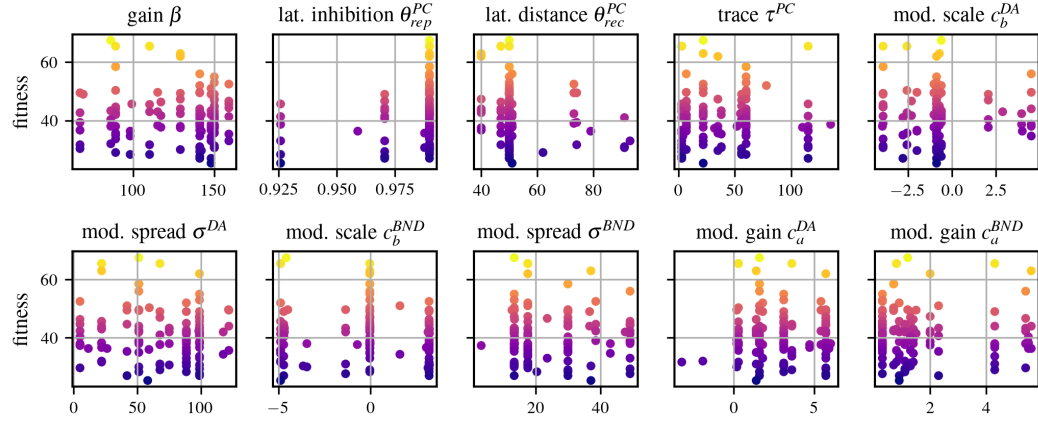


Figure 7: **Distribution of evolved parameters** - Results relative to the last generation, from a run with population size of 128 individuals.

685 **1. Claims**

686 Question: Do the main claims made in the abstract and introduction accurately reflect the
687 paper's contributions and scope?

688 Answer: [Yes]

689 Justification: the methods, experiments, and results match what is stated in the abstract and
690 introduction

691 Guidelines:

- 692 • The answer NA means that the abstract and introduction do not include the claims
693 made in the paper.
- 694 • The abstract and/or introduction should clearly state the claims made, including the
695 contributions made in the paper and important assumptions and limitations. A No or
696 NA answer to this question will not be perceived well by the reviewers.
- 697 • The claims made should match theoretical and experimental results, and reflect how
698 much the results can be expected to generalize to other settings.
- 699 • It is fine to include aspirational goals as motivation as long as it is clear that these goals
700 are not attained by the paper.

701 **2. Limitations**

702 Question: Does the paper discuss the limitations of the work performed by the authors?

703 Answer: [Yes]

704 Justification: the limits of the model architecture and of the experiments are taken into
705 account within the Methods and Discussion sections.

706 Guidelines:

- 707 • The answer NA means that the paper has no limitation while the answer No means that
708 the paper has limitations, but those are not discussed in the paper.
- 709 • The authors are encouraged to create a separate "Limitations" section in their paper.
- 710 • The paper should point out any strong assumptions and how robust the results are to
711 violations of these assumptions (e.g., independence assumptions, noiseless settings,
712 model well-specification, asymptotic approximations only holding locally). The authors
713 should reflect on how these assumptions might be violated in practice and what the
714 implications would be.
- 715 • The authors should reflect on the scope of the claims made, e.g., if the approach was
716 only tested on a few datasets or with a few runs. In general, empirical results often
717 depend on implicit assumptions, which should be articulated.
- 718 • The authors should reflect on the factors that influence the performance of the approach.
719 For example, a facial recognition algorithm may perform poorly when image resolution
720 is low or images are taken in low lighting. Or a speech-to-text system might not be
721 used reliably to provide closed captions for online lectures because it fails to handle
722 technical jargon.
- 723 • The authors should discuss the computational efficiency of the proposed algorithms
724 and how they scale with dataset size.
- 725 • If applicable, the authors should discuss possible limitations of their approach to
726 address problems of privacy and fairness.
- 727 • While the authors might fear that complete honesty about limitations might be used by
728 reviewers as grounds for rejection, a worse outcome might be that reviewers discover
729 limitations that aren't acknowledged in the paper. The authors should use their best
730 judgment and recognize that individual actions in favor of transparency play an impor-
731 tant role in developing norms that preserve the integrity of the community. Reviewers
732 will be specifically instructed to not penalize honesty concerning limitations.

733 **3. Theory assumptions and proofs**

734 Question: For each theoretical result, does the paper provide the full set of assumptions and
735 a complete (and correct) proof?

736 Answer: [Yes]

737 Justification: the methodological premises of each experiment, with its result, are mentioned
738 and discussed, in the Results and Discussion section.

739 Guidelines:

- 740 • The answer NA means that the paper does not include theoretical results.
741 • All the theorems, formulas, and proofs in the paper should be numbered and cross-
742 referenced.
743 • All assumptions should be clearly stated or referenced in the statement of any theorems.
744 • The proofs can either appear in the main paper or the supplemental material, but if
745 they appear in the supplemental material, the authors are encouraged to provide a short
746 proof sketch to provide intuition.
747 • Inversely, any informal proof provided in the core of the paper should be complemented
748 by formal proofs provided in appendix or supplemental material.
749 • Theorems and Lemmas that the proof relies upon should be properly referenced.

750 4. Experimental result reproducibility

751 Question: Does the paper fully disclose all the information needed to reproduce the main ex-
752 perimental results of the paper to the extent that it affects the main claims and/or conclusions
753 of the paper (regardless of whether the code and data are provided or not)?

754 Answer: [Yes]

755 Justification: the Appendix, together with the Methods section, reports enough information
756 for a solid understanding of the functioning model and the experiments.

757 Guidelines:

- 758 • The answer NA means that the paper does not include experiments.
759 • If the paper includes experiments, a No answer to this question will not be perceived
760 well by the reviewers: Making the paper reproducible is important, regardless of
761 whether the code and data are provided or not.
762 • If the contribution is a dataset and/or model, the authors should describe the steps taken
763 to make their results reproducible or verifiable.
764 • Depending on the contribution, reproducibility can be accomplished in various ways.
765 For example, if the contribution is a novel architecture, describing the architecture fully
766 might suffice, or if the contribution is a specific model and empirical evaluation, it may
767 be necessary to either make it possible for others to replicate the model with the same
768 dataset, or provide access to the model. In general, releasing code and data is often
769 one good way to accomplish this, but reproducibility can also be provided via detailed
770 instructions for how to replicate the results, access to a hosted model (e.g., in the case
771 of a large language model), releasing of a model checkpoint, or other means that are
772 appropriate to the research performed.
773 • While NeurIPS does not require releasing code, the conference does require all submis-
774 sions to provide some reasonable avenue for reproducibility, which may depend on the
775 nature of the contribution. For example
776 (a) If the contribution is primarily a new algorithm, the paper should make it clear how
777 to reproduce that algorithm.
778 (b) If the contribution is primarily a new model architecture, the paper should describe
779 the architecture clearly and fully.
780 (c) If the contribution is a new model (e.g., a large language model), then there should
781 either be a way to access this model for reproducing the results or a way to reproduce
782 the model (e.g., with an open-source dataset or instructions for how to construct
783 the dataset).
784 (d) We recognize that reproducibility may be tricky in some cases, in which case
785 authors are welcome to describe the particular way they provide for reproducibility.
786 In the case of closed-source models, it may be that access to the model is limited in
787 some way (e.g., to registered users), but it should be possible for other researchers
788 to have some path to reproducing or verifying the results.

789 5. Open access to data and code

790 Question: Does the paper provide open access to the data and code, with sufficient instruc-
791 tions to faithfully reproduce the main experimental results, as described in supplemental
792 material?

793 Answer: [Yes]

794 Justification: the codebase of this work is publicly available on github, and includes all
795 script behing the model and experiments.

796 Guidelines:

- 797 • The answer NA means that paper does not include experiments requiring code.
- 798 • Please see the NeurIPS code and data submission guidelines (<https://nips.cc/public/guides/CodeSubmissionPolicy>) for more details.
- 800 • While we encourage the release of code and data, we understand that this might not be
801 possible, so “No” is an acceptable answer. Papers cannot be rejected simply for not
802 including code, unless this is central to the contribution (e.g., for a new open-source
803 benchmark).
- 804 • The instructions should contain the exact command and environment needed to run to
805 reproduce the results. See the NeurIPS code and data submission guidelines (<https://nips.cc/public/guides/CodeSubmissionPolicy>) for more details.
- 806 • The authors should provide instructions on data access and preparation, including how
807 to access the raw data, preprocessed data, intermediate data, and generated data, etc.
- 808 • The authors should provide scripts to reproduce all experimental results for the new
809 proposed method and baselines. If only a subset of experiments are reproducible, they
810 should state which ones are omitted from the script and why.
- 811 • At submission time, to preserve anonymity, the authors should release anonymized
812 versions (if applicable).
- 813 • Providing as much information as possible in supplemental material (appended to the
814 paper) is recommended, but including URLs to data and code is permitted.

816 6. Experimental setting/details

817 Question: Does the paper specify all the training and test details (e.g., data splits, hyper-
818 parameters, how they were chosen, type of optimizer, etc.) necessary to understand the
819 results?

820 Answer: [Yes]

821 Justification: the Methods, Results, and Appendix section include the necessary details
822 accounting for the results.

823 Guidelines:

- 824 • The answer NA means that the paper does not include experiments.
- 825 • The experimental setting should be presented in the core of the paper to a level of detail
826 that is necessary to appreciate the results and make sense of them.
- 827 • The full details can be provided either with the code, in appendix, or as supplemental
828 material.

829 7. Experiment statistical significance

830 Question: Does the paper report error bars suitably and correctly defined or other appropriate
831 information about the statistical significance of the experiments?

832 Answer: [Yes]

833 Justification: the statistical significance of the tests is reported in the figures.

834 Guidelines:

- 835 • The answer NA means that the paper does not include experiments.
- 836 • The authors should answer “Yes” if the results are accompanied by error bars, confi-
837 dence intervals, or statistical significance tests, at least for the experiments that support
838 the main claims of the paper.
- 839 • The factors of variability that the error bars are capturing should be clearly stated (for
840 example, train/test split, initialization, random drawing of some parameter, or overall
841 run with given experimental conditions).

- The method for calculating the error bars should be explained (closed form formula, call to a library function, bootstrap, etc.)
- The assumptions made should be given (e.g., Normally distributed errors).
- It should be clear whether the error bar is the standard deviation or the standard error of the mean.
- It is OK to report 1-sigma error bars, but one should state it. The authors should preferably report a 2-sigma error bar than state that they have a 96% CI, if the hypothesis of Normality of errors is not verified.
- For asymmetric distributions, the authors should be careful not to show in tables or figures symmetric error bars that would yield results that are out of range (e.g. negative error rates).
- If error bars are reported in tables or plots, The authors should explain in the text how they were calculated and reference the corresponding figures or tables in the text.

855 8. Experiments compute resources

856 Question: For each experiment, does the paper provide sufficient information on the com-
 857 puter resources (type of compute workers, memory, time of execution) needed to reproduce
 858 the experiments?

859 Answer: [Yes]

860 Justification: the specification of the computational resources is mentioned.

861 Guidelines:

- The answer NA means that the paper does not include experiments.
- The paper should indicate the type of compute workers CPU or GPU, internal cluster, or cloud provider, including relevant memory and storage.
- The paper should provide the amount of compute required for each of the individual experimental runs as well as estimate the total compute.
- The paper should disclose whether the full research project required more compute than the experiments reported in the paper (e.g., preliminary or failed experiments that didn't make it into the paper).

870 9. Code of ethics

871 Question: Does the research conducted in the paper conform, in every respect, with the
 872 NeurIPS Code of Ethics <https://neurips.cc/public/EthicsGuidelines>?

873 Answer: [Yes]

874 Justification: the paper conforms to the NeurIPS Code of Ethics.

875 Guidelines:

- The answer NA means that the authors have not reviewed the NeurIPS Code of Ethics.
- If the authors answer No, they should explain the special circumstances that require a deviation from the Code of Ethics.
- The authors should make sure to preserve anonymity (e.g., if there is a special consideration due to laws or regulations in their jurisdiction).

881 10. Broader impacts

882 Question: Does the paper discuss both potential positive societal impacts and negative
 883 societal impacts of the work performed?

884 Answer: [NA]

885 Justification: to our knowledge, the paper does not involve nor impact any relevant societal
 886 aspect, for the main reason that it solely concerns computational modelling of neuronal and
 887 behavioural dynamics.

888 Guidelines:

- The answer NA means that there is no societal impact of the work performed.
- If the authors answer NA or No, they should explain why their work has no societal impact or why the paper does not address societal impact.

- 892 • Examples of negative societal impacts include potential malicious or unintended uses
893 (e.g., disinformation, generating fake profiles, surveillance), fairness considerations
894 (e.g., deployment of technologies that could make decisions that unfairly impact specific
895 groups), privacy considerations, and security considerations.
- 896 • The conference expects that many papers will be foundational research and not tied
897 to particular applications, let alone deployments. However, if there is a direct path to
898 any negative applications, the authors should point it out. For example, it is legitimate
899 to point out that an improvement in the quality of generative models could be used to
900 generate deepfakes for disinformation. On the other hand, it is not needed to point out
901 that a generic algorithm for optimizing neural networks could enable people to train
902 models that generate Deepfakes faster.
- 903 • The authors should consider possible harms that could arise when the technology is
904 being used as intended and functioning correctly, harms that could arise when the
905 technology is being used as intended but gives incorrect results, and harms following
906 from (intentional or unintentional) misuse of the technology.
- 907 • If there are negative societal impacts, the authors could also discuss possible mitigation
908 strategies (e.g., gated release of models, providing defenses in addition to attacks,
909 mechanisms for monitoring misuse, mechanisms to monitor how a system learns from
910 feedback over time, improving the efficiency and accessibility of ML).

911 11. Safeguards

912 Question: Does the paper describe safeguards that have been put in place for responsible
913 release of data or models that have a high risk for misuse (e.g., pretrained language models,
914 image generators, or scraped datasets)?

915 Answer: [NA]

916 Justification: this work does not involve any high risk data or models, and thus safeguards
917 have not been deemed necessary.

918 Guidelines:

- 919 • The answer NA means that the paper poses no such risks.
- 920 • Released models that have a high risk for misuse or dual-use should be released with
921 necessary safeguards to allow for controlled use of the model, for example by requiring
922 that users adhere to usage guidelines or restrictions to access the model or implementing
923 safety filters.
- 924 • Datasets that have been scraped from the Internet could pose safety risks. The authors
925 should describe how they avoided releasing unsafe images.
- 926 • We recognize that providing effective safeguards is challenging, and many papers do
927 not require this, but we encourage authors to take this into account and make a best
928 faith effort.

929 12. Licenses for existing assets

930 Question: Are the creators or original owners of assets (e.g., code, data, models), used in
931 the paper, properly credited and are the license and terms of use explicitly mentioned and
932 properly respected?

933 Answer: [Yes]

934 Justification: the creators, credits, and licensed have been properly mentioned and addressed.

935 Guidelines:

- 936 • The answer NA means that the paper does not use existing assets.
- 937 • The authors should cite the original paper that produced the code package or dataset.
- 938 • The authors should state which version of the asset is used and, if possible, include a
939 URL.
- 940 • The name of the license (e.g., CC-BY 4.0) should be included for each asset.
- 941 • For scraped data from a particular source (e.g., website), the copyright and terms of
942 service of that source should be provided.

- 943 • If assets are released, the license, copyright information, and terms of use in the
944 package should be provided. For popular datasets, paperswithcode.com/datasets
945 has curated licenses for some datasets. Their licensing guide can help determine the
946 license of a dataset.
947 • For existing datasets that are re-packaged, both the original license and the license of
948 the derived asset (if it has changed) should be provided.
949 • If this information is not available online, the authors are encouraged to reach out to
950 the asset's creators.

951 **13. New assets**

952 Question: Are new assets introduced in the paper well documented and is the documentation
953 provided alongside the assets?

954 Answer: [NA]

955 Justification: no new asset has been introduced, other than the code used for building and
956 testing the model.

957 Guidelines:

- 958 • The answer NA means that the paper does not release new assets.
959 • Researchers should communicate the details of the dataset/code/model as part of their
960 submissions via structured templates. This includes details about training, license,
961 limitations, etc.
962 • The paper should discuss whether and how consent was obtained from people whose
963 asset is used.
964 • At submission time, remember to anonymize your assets (if applicable). You can either
965 create an anonymized URL or include an anonymized zip file.

966 **14. Crowdsourcing and research with human subjects**

967 Question: For crowdsourcing experiments and research with human subjects, does the paper
968 include the full text of instructions given to participants and screenshots, if applicable, as
969 well as details about compensation (if any)?

970 Answer: [NA]

971 Justification: the paper does not involve crowdsourcing nor human subjects.

972 Guidelines:

- 973 • The answer NA means that the paper does not involve crowdsourcing nor research with
974 human subjects.
975 • Including this information in the supplemental material is fine, but if the main contribu-
976 tion of the paper involves human subjects, then as much detail as possible should be
977 included in the main paper.
978 • According to the NeurIPS Code of Ethics, workers involved in data collection, curation,
979 or other labor should be paid at least the minimum wage in the country of the data
980 collector.

981 **15. Institutional review board (IRB) approvals or equivalent for research with human
982 subjects**

983 Question: Does the paper describe potential risks incurred by study participants, whether
984 such risks were disclosed to the subjects, and whether Institutional Review Board (IRB)
985 approvals (or an equivalent approval/review based on the requirements of your country or
986 institution) were obtained?

987 Answer: [NA]

988 Justification: the paper does not involve crowdsourcing nor human subject.

989 Guidelines:

- 990 • The answer NA means that the paper does not involve crowdsourcing nor research with
991 human subjects.
992 • Depending on the country in which research is conducted, IRB approval (or equivalent)
993 may be required for any human subjects research. If you obtained IRB approval, you
994 should clearly state this in the paper.

- 995 • We recognize that the procedures for this may vary significantly between institutions
996 and locations, and we expect authors to adhere to the NeurIPS Code of Ethics and the
997 guidelines for their institution.
998 • For initial submissions, do not include any information that would break anonymity (if
999 applicable), such as the institution conducting the review.

1000 **16. Declaration of LLM usage**

1001 Question: Does the paper describe the usage of LLMs if it is an important, original, or
1002 non-standard component of the core methods in this research? Note that if the LLM is used
1003 only for writing, editing, or formatting purposes and does not impact the core methodology,
1004 scientific rigorousness, or originality of the research, declaration is not required.

1005 Answer: [NA]

1006 Justification: the usage of LLMs was limited to writing, editing, and formatting purposes.
1007 There was no usage for developing the model or the research background.

1008 Guidelines:

- 1009 • The answer NA means that the core method development in this research does not
1010 involve LLMs as any important, original, or non-standard components.
1011 • Please refer to our LLM policy (<https://neurips.cc/Conferences/2025/LLM>)
1012 for what should or should not be described.